Mater. Res. Soc. Proc. Vol. 594, Fall 99 Symp. V: Thin Films-Stresses and Mechanical Properties VIII

SUPERLAYER RESIDUAL STRESS EFFECT ON THE INDENTATION ADHESION MEASUREMENTS

Alex A. Volinsky, Neville R. Moody* and William W. Gerberich
University of Minnesota, Dept. of Chemical Engineering and Materials Science, Minneapolis, MN 55455, volinsky@cems.umn.edu
* Sandia National Laboratories, Livermore, CA 94550

ABSTRACT

The practical work of adhesion has been measured in thin aluminum films as a function of film thickness and residual stress. These films were sputter deposited onto thermally oxidized silicon wafers followed by sputter deposition of a one micron thick W superlayer. The superlayer deposition parameters were controlled to produce either a compressive residual stress of 1 GPa or a tensile residual stress of 100 MPa. Nanoindentation testing was then used to induce delamination and a mechanics based model for circular blister formation was used to determine practical works of adhesion. The resulting measured works of adhesion for all films between 100 nm and 1 μm thick was 30 J/m^2 regardless of superlayer stress. However, films with the compressively stressed superlayers produced larger blisters than films with tensile stressed superlayers. In addition, these films were susceptible to radial cracking producing a high variability in average adhesion values.

INTRODUCTION

Several researchers have used nanoindentation to examine the effect of residual stress on the modulus and hardness of bulk materials and of thin films [1-4]. It has also been used to study adhesion of thin metallic and ceramic films where residual stresses drive delamination and failure. However, little work has been done using this technique to study adhesion of ductile thin films. These films cannot store enough strain energy or transmit forces of sufficient strength to the film-substrate interface for crack initiation and propagation. Recent work shows that deposition of a highly stressed superlayer onto thin ductile copper films can provide the stresses required for delamination during indentation testing [7, 9, 10]. Based on this work, we have employed nanoindentation in a study of compressive and tensile residual stresses created during sputter deposition of tungsten superlayers on the adhesion of thin ductile aluminum films.

EXPERIMENT

All thin film processing was conducted in a Class 10 clean room environment. Silicon <100> wafers (100 mm in diameter, 0.5 mm thick) were thermally oxidized at 1100 °C in steam to grow 3 μm of SiO_2. Oxide thickness was measured with a Nanoscope Ellipsometer. Al films from 40 nm to 3.2 μm thick were then deposited onto the oxidized substrates in a Perkin-Elmer DC Magnetron sputtering apparatus. The base pressure of the system was 1 μTorr, and the Ar flow was 10 sccm, which corresponded to 6 mTorr Ar pressure. For Al films from 500 nm to 3.2 μm thick, 5000 Watts of power was applied to the target (Al-2% Si, w/o); for thinner films the sputtering power was reduced to 1000 Watts. Substrate table rotation was used to achieve uniform film thickness and structure. The maximum temperature during film deposition reached 100 °C for the longest deposition run of 3 μm Al, after which the system was cooled for one hour without breaking vacuum. Film thickness was measured using a DEKTAK surface profiler. Using the wafer curvature technique and Stoney's equation [11], residual stresses measured were

tensile and ranged from 100 to 200 MPa . Sheet resistance of the Al films was measured with a Veeco Instruments Inc. 4-point probe. Reflectance was measured with a Nanometrics Nanospec film thickness measurement system in the reflectance mode, taking a Si wafer as a 100% reflectance reference. As expected, both properties decreased with the film thickness (Figure 1). Al films of 1, 2 and 3 μm thick appeared to produce more scatter than the others due to the higher surface roughness and thicker oxide layer. Two sets of Al films of all eight thicknesses were coated with two different W superlayers in a 2400 Perkin-Elmer RF sputtering apparatus. The residual stress in sputter deposited films was controlled by varying the working gas pressure [12,13]. For the first superlayer deposition run the Ar pressure was held at 7.7 mTorr, which produced a compressive residual stress of 1 GPa in the W superlayer. For the second run, the Ar pressure was held at 6 mTorr, which produced a tensile residual stress of 100 MPa. The stresses were measured using wafer curvature.

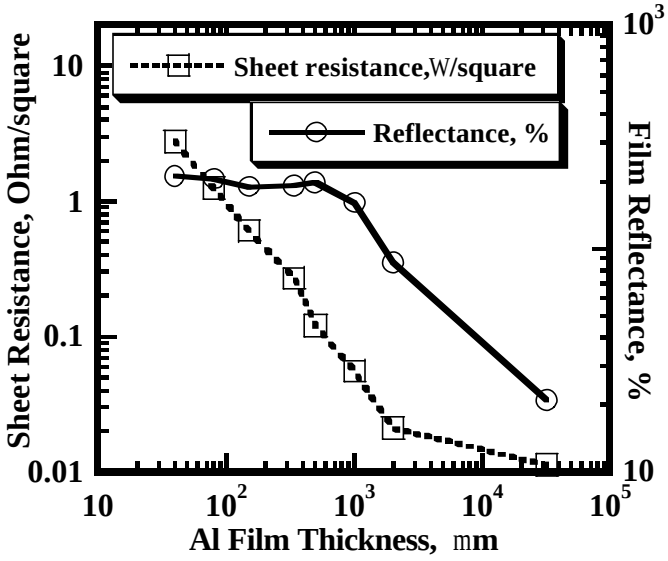

Figure 1. Sheet resistance and reflectance of Al films as a function of film thickness.

All test structures were indented using a conical 90° angle 1 μm radius tip on a Nanoindenter II to six different loads: 25, 50, 100, 200, 400 and 600 mN. There were 3 indents at each load, giving a total of 18 indents for each film thickness. Load-displacement curves were recorded continuously during the tests (Figure 2a and Figure 3a).

ADHESION CALCULATIONS

According to the analysis of Marshall and Evans [6], the strain energy release rate (practical work of adhesion) is related to the indentation stress, s_I, thin film residual stress, s_R and the buckling stress, s_B:

$$G \equiv \frac{h s_I^2 (1-n^2)}{2E} + (1-a)\frac{h s_R^2 (1-n)}{E} - (1-a)\frac{h(s_I - s_B)^2 (1-n)}{E} \qquad (1),$$

where E is the film's Young's modulus, and n is its Poisson ratio. The parameter α is equal to 1 when the film is not buckled, and $0 < \alpha < 1$ otherwise. Note that for the non-buckled film configuration, it is only the indentation stress that drives delamination. The residual stress comes into play only if the film is buckled. Originally equation (1) was derived for the case of compressive residual stresses in the film. The same approach can be used for the case of tensile residual stresses.

Kriese et al [7] modified the analysis, providing solutions of each term in equation (1) for multilayers. Besides the indenter tip geometry and the properties of each layer such as film thickness, residual stress, and elastic modulus, there are two variables that are found experimentally for each adhesion indentation test: the delamination blister radius (x) and the residual indentation depth (d_{res}). The residual indentation depth is found from the load-

displacement curve by fitting 65% of its unloading portion with the Oliver-Pharr equation [8]. Knowing the indenter tip geometry, the indentation volume (V_I) and thus the indentation stress (s_I) can be calculated. These values were then used with indentation depths and blister radii to calculate strain energy release rates.

SUPERLAYER RESIDUAL STRESS

We see that in the case of the tensile stressed superlayer, the indenter goes deeper into the films for a given load, in agreement with experimental observations and FEM predictions for both bulk materials and thin films [1-5]. This effect is observed on all eight Al film thicknesses (Figure 2a and Figure 3a). For thin film systems under 1 μm thick, this results in the maximum indentation loads on the order of one mN. For the delamination tests, the first deviation in the loading slope of the load-displacement curve is observed at the depth of 200 nm, with a 10 mN load required for a 40 nm thick Al film (Figure 2a). Since a 200 nm depth is still within the spherical region of the indenter tip (R_P = 1 μm), the corresponding pressure is 24 GPa.

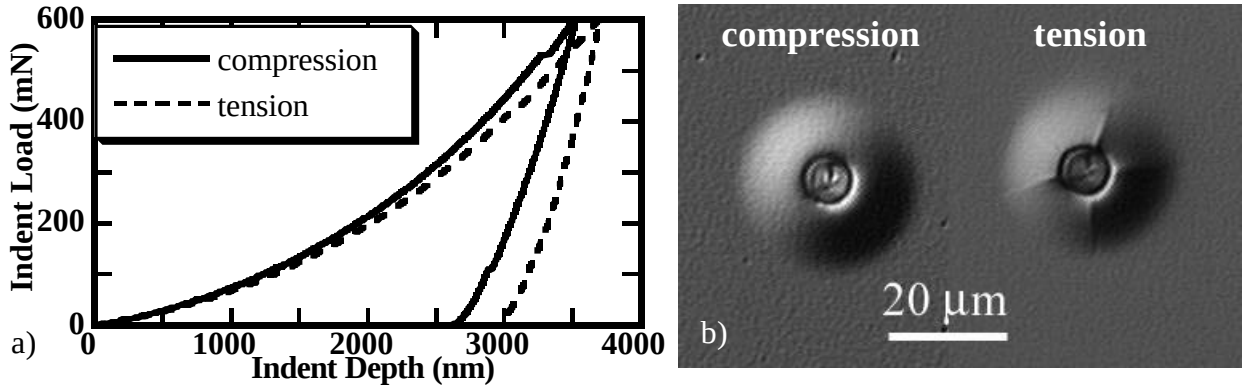

Figure 2. Load-displacement curves (a) and corresponding blister delaminations (b) for a 40 nm thick Al film with compressive and tensile W superlayers.

Zagrebelny and Carter [3] deposited silicate-glass films on pre-bent and strained sapphire substrates to control the residual stress in their films. Here tensile and compressive residual stresses of 0.4 GPa were achieved by substrate bending. Compared to the superlayer indentation, a similar result was observed qualitatively in terms of the loading behavior. The first deviation in the loading slope of their load-displacement curve was observed at a depth of 10 nm with a 0.2 mN corresponding load for a 200 nm thick glass film. Since a sharp Berkovich tip was used (R_{tip}=80 nm), the corresponding indenter pressure appeared to be 120 GPa, well above what would normally be expected even in a sapphire substrate. It is suspected that even in these relatively brittle materials residual stress affects the resulting contact area through its effect on plastic flow giving the deviation observed.

The residual stress in the case of the superlayer indentations was not achieved by substrate bending as above but rather by changing the sputter deposition parameters. As a consequence, the resulting microstructure, density and properties of the superlayer W films were expected to differ between films in tension and compression. They were also expected to exhibit a difference in load-displacement behavior.

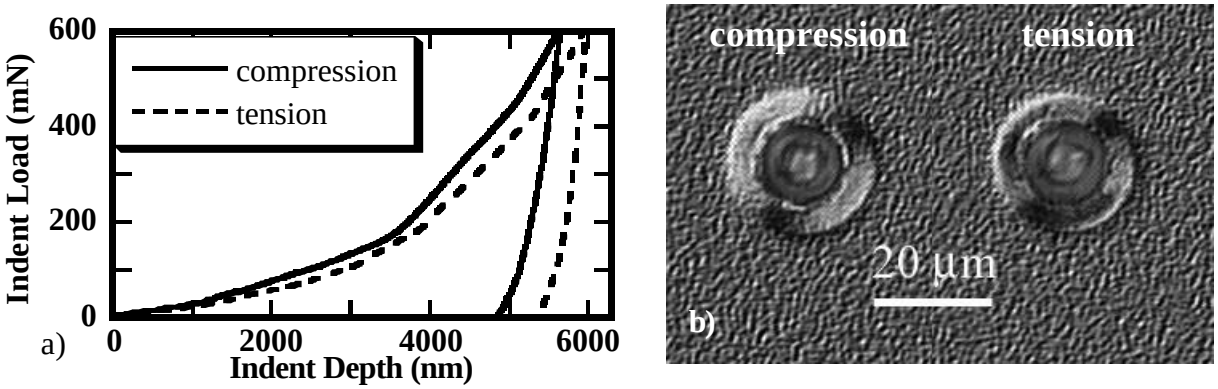

Figure 3. Load-displacement curves (a) and corresponding blister delaminations (b) for a 2 μm thick Al film with compressive and tensile W superlayers.

It is worthwhile to note that indentation adhesion measurements involve film debonding from the substrate, which occurs during the loading of the indenter into the film. The loading portion of the load-displacement curve also represents the multilayer compliance, which appears to be higher in the tensile case. Thin aluminum films with tensile stressed superlayers produce radial cracks emanating from the indentations (Figure 2b). For the same indentation load, films with radial cracks around the indenter create a larger contact area than films without cracks (Figure 4). On the other hand, radial cracking combines with buckling to relieve the residual tensile stresses, whereas buckling is the only means to relieve residual compressive stresses. Given these differences, one should consider how these might affect the actual adhesion measurements.

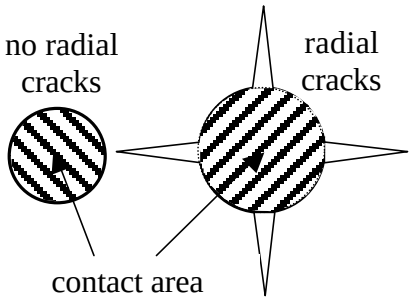

Figure 4. Radial cracking contribution to the increase in the contact area.

DISCUSSION

The practical work of adhesion, W_p consists of the thermodynamic (also called true) work of adhesion, W_T, and other energy dissipation terms in the film (U_f) and in the substrate (U_s):

$$W_P = W_T + U_f + U_s \qquad (2)$$

In the case of a ductile thin film (Cu or Al) on a hard substrate (Si/SiO_2), plastic deformation of the film will contribute most of the energy comprising the practical work of adhesion, as shown in a previous study of copper films [9]. The amount of plastic deformation at the crack tip and the practical work of adhesion increased with film thickness. Al thin film adhesion as a function of Al film thickness is presented in Figure 5 for both types of W superlayers. With one exception at a thickness of 40 nm, there appears to be almost no thickness effect on the practical work of adhesion (30 J/m^2) of Al films up to 1 μm thick. Blister delaminations appear to be smaller and the residual indentation greater for a tensile stressed superlayer (Figure 2b). Since the indentation depth is always larger with a tensile stressed W superlayer, one may expect such films to have a higher practical work of adhesion than films with a compressively stressed superlayer. However, this appears to not be the case, since

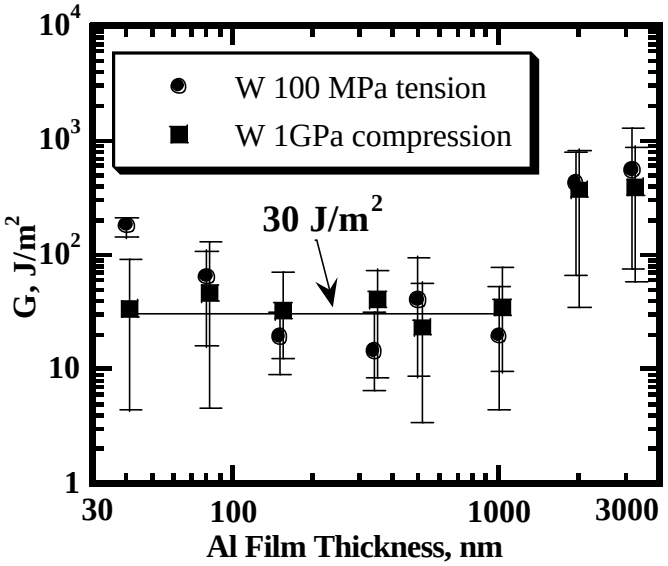

adhesion values start to overlap for 80 and 150 nm thick Al films with both tensile and compressive superlayers. The difference in the practical work of adhesion of nearly 150 J/m^2 for 40 nm thick Al films is also difficult to justify by radial cracking as well, since this effect becomes negligible at greater Al thicknesses.

Figure 5. Al thin film adhesion with residual tensile and compressive residual stresses in the W superlayer. (Data points are shifted in the x-axis for clearity).

Adhesion values converge for both residual tensile and compressive W superlayers for 2 and 3.2 μm thick Al films, reaching on average an extremely large value of 500 J/m^2. Though Ritchie et al [15] measured Al_2O_3/Al toughness of 65 to 400 J/m^2 using a 4-point bend test, we believe that such high values are unreasonable for a 3.2 μm thick Al film. For these films, the high values can be attributed to crack tip interaction effects from overlap of the plastic zones around the indenter and crack tip [9]. To briefly illustrate the effect, Figure 6 shows the normalized strain energy release rate as a function of distance from the indenter for both plane strain and plane stress. The plane strain solution from Vlassak et al [14] is applicable for a wedge indenter, plane strain conditions. A corresponding plane stress plot (Figure 6b) is obtained by varying both the indentation depth and the blister diameter using the bilayer solution by Kriese et al [7]. Both solutions are normalized by the appropriate strain energy release rate due to just the residual stress:

$$G_0 = \frac{s_{resW}^2 h}{2E_W} \text{ for plane stress, } G_0 = \frac{s_{resW}^2 h(1-n_W^2)}{2E_W} \text{ for plane strain} \qquad (3)$$

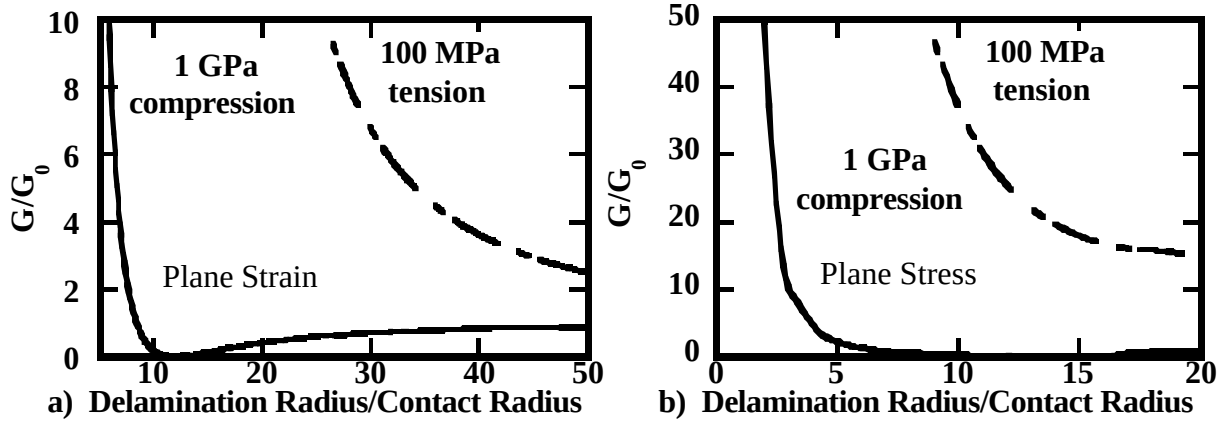

Figure 6. Plane strain a) [14] and plane stress b) [7] normalized strain energy release rate as a function of distance from the indentation for films with residual tensile and compressive residual stresses.

The blister to the indenter contact diameter ratio has to be much greater in case of a tensile W superlayer compared to compression to avoid this tip interaction effect. Since the radii

ratio is only about three for thick Al films (Figure 3b), this tip interaction effect is present regardless of the magnitude of the superlayer stress. The only way to solve the problem would be to use a thicker W superlayer, which will store higher elastic energies available for delamination. Given the same test conditions, a compressive residual stress in the superlayer is preferred. Here, the compressive residual stresses in the superlayer are being added to the indentation stress. On the other hand, the indenter has to overcome the tensile residual stress to achieve sufficient compression before a crack can nucleate and grow at the interface. The current analysis does not account for radial cracking, as well as for residual stresses prior to film buckling; both may have an effect on the multilayer buckling stress threshold.

CONCLUSIONS

The practical works of adhesion for Al thin films of different thicknesses have been measured using the superlayer indentation technique. Compressive and tensile residual stresses in the superlayer were achieved by changing the sputtering deposition parameters. Films with the tensile W superlayer exhibited radial cracking up to 1 μm thick Al film. The greatest difference of 150 J/m^2 in the measured adhesion values was observed on a 40 nm Al film. In general, compressive residual stresses in the superlayer are preferred. It appears that a tip interaction effect may be present in all measurements, and this will be further addressed in future work.

ACKNOWLEDGEMENTS

The authors would like to acknowledge support for this work by the Center for Interfacial Engineering at the University of Minnesota under grant NSF/CDR-8721551, the Department of Energy under DOE contract DE-FG02/96ER45574. A.A. Volinsky and N.R. Moody also acknowledge support through DOE contract DE-AC04-94AL85000. The assistance of M.K. Sanovskaya, D.E. Kramer, N.I. Tymiak, W.M. Clift and B.E. Mills, D.E. McLean and D. Medlin is appreciated. The assistance of Dr. J.C. Nelson from the Center for Interfacial Engineering and Microtechnology Laboratory staff at the University of Minnesota is also gratefully appreciated.

REFERENCES

1. T.Y. Tsui, W.C. Oliver, G.M. Pharr, J. Mater. Res., **11**(3), 752-759, 1996
2. A. Bolshakov, W.C. Oliver, G.M. Pharr, J. Mater. Res., **11**(3), 760-768, 1996
3. A.V. Zagrebelny, C.B. Carter, Scripta Mater., **37**(12), 1869-1875, 1997
4. A.V. Zagrebelny, C.B. Carter, Philosophical Magazine A, **79**(4), 835-845, 1998
5. S. Suresh, A.E. Giannakopoulos, Acta Materialia, **46**(16), 5755-5767, 1998
6. D.B. Marshall, A.G. Evans, J. Appl. Phys. **56**(10), 2632-2638, 1984
7. M.D. Kriese, W.W. Gerberich, N.R. Moody, J. Mater. Res., **14**(7), 3007-3018, 1998
8. W.C. Oliver and G.M. Pharr, J. Mater. Res., **7**, 1564-1583, 1992
9. A.A. Volinsky, N.I. Tymiak, M.D. Kriese, W.W. Gerberich, Mat. Res. Soc. Symp. Proc. **539**, 277-290, 1999
10. N.I. Tymiak, A.A. Volinsky, M.D. Kriese, S.A. Downs, W.W. Gerberich, accepted for publication in Metallurgical Transactions, 1999
11. G.G. Stoney, Proc.Roy.Soc.Lond. **A82,** 72, 1909
12. J.A. Thornton, D.W. Hoffman, Thin Solid Films, **171**(1), 5-31, 1989
13. M. Ohring, The Materials Science of Thin Films, Academic Press, 1992
14. J.J. Vlassak, M.D. Drory, W.D. Nix, J. Mater. Res., **12**(7), 1900-1910, 1997
15. R.O. Ritchie, R.M. Cannon, B.J. Dalgleish, R.H. Dauskardt, J.M. McNaney, Mater. Sci. and Eng., **A166,** 221-235, 1993